The Diffuse Auroral Eraser

Riley N Troyer[1], Allison N Jaynes[1], Sarah L Jones[2], David J. Knudsen[3], and Trond Steinar Trondsen[3]

[1]University of Iowa
[2]Goddard Space Flight Center (NASA)
[3]University of Calgary

May 23, 2023

Abstract

The source of diffuse aurora has been widely studied and linked to electron cyclotron harmonic (ECH) and upper-band chorus (UBC) waves. It is known that these waves scatter 100s of eV to 10s of keV electrons from the plasma sheet, but the relative contribution of each wave type is still an open question. In this paper, we report on a new structured diffuse aurora feature observed on March 15, 2002 that could help further our understanding. This feature is characterized by four phases: (1) the initial phase exhibiting regular diffuse aurora, (2) the brightening phase, where a stripe of diffuse aurora rapidly brightens, (3) the eraser phase, where the stripe dims to below its initial state, and (4) the recovery phase, where the diffuse aurora returns to its original brightness. Using a superposed epoch analysis of 22 events, we calculate the average recovery phase time to be 20 seconds, although this varies widely between events. We hypothesize that the process responsible for these auroral eraser events could be an interaction between ECH and chorus waves.

The Diffuse Auroral Eraser

R. N. Troyer [1], A. N. Jaynes [1], S. L. Jones [2], D. J. Knudsen [3], T. Trondsen [4]

[1]Department of Physics and Astronomy, University of Iowa
[2]NASA Goddard Space Flight Center
[3]Department of Physics and Astronomy, University of Calgary
[4]Keo Scientific Ltd.

Key Points:

- We identify a new feature, called a diffuse auroral eraser, which has never been reported on and occurred during low magnetic activity.
- An auroral eraser starts as diffuse aurora that brightens, dims to lower than its initial level, then recovers to its initial brightness.
- We found the average recovery time to be 20 seconds with a 13 second standard deviation.

Corresponding author: Riley Troyer, `riley-troyer@uiowa.edu`

Abstract

The source of diffuse aurora has been widely studied and linked to electron cyclotron harmonic (ECH) and upper-band chorus (UBC) waves. It is known that these waves scatter 100s of eV to 10s of keV electrons from the plasma sheet, but the relative contribution of each wave type is still an open question. In this paper, we report on a new structured diffuse aurora feature observed on March 15, 2002 that could help further our understanding. This feature is characterized by four phases: (1) the initial phase exhibiting regular diffuse aurora, (2) the brightening phase, where a stripe of diffuse aurora rapidly brightens, (3) the eraser phase, where the stripe dims to below its initial state, and (4) the recovery phase, where the diffuse aurora returns to its original brightness. Using a superposed epoch analysis of 22 events, we calculate the average recovery phase time to be 20 seconds, although this varies widely between events. We hypothesize that the process responsible for these auroral eraser events could be an interaction between ECH and chorus waves.

Plain Language Summary

Aurora are caused by electrons from within the magnetic bubble that surrounds Earth, called that magnetosphere. Sometimes these electrons are deposited into our upper atmosphere, producing light. This process can also transfer large amounts of energy from the magnetosphere to the atmosphere, thus potentially affecting the climate. Pictures of the aurora usually depict discrete green curtains, but this is not the only type of aurora. Diffuse aurora is another, which look like a faint glow over large portions of the sky. Diffuse aurora are extremely common, but not well understood. We have found a new process within diffuse aurora that could improve our understanding. We call them diffuse auroral eraser events. We found these events in a movie taken the night of March 15, 2002 in Churchill, MB, Canada. They appear as a section of diffuse aurora that rapidly brightens, then disappears and also erases the background aurora. Then, over the course of several tens of seconds, the diffuse aurora recovers to its original brightness. We calculated the average recovery time by overlaying plots of brightness from each of the 22 events that we found. This average time was 20 seconds, although it varied widely between individual events.

1 Introduction

Originally referred to as mantle aurora, diffuse aurora appears as a faint glow, just visible to the naked eye, and spread across a large portion of the sky (Lui et al., 1973). The location of this aurora occurs equatorward of the discrete auroral oval and usually peaks in activity and brightness after magnetic midnight. This typically corresponds to between 60° and 75° corrected geomagnetic latitude, depending on the solar cycle and geomagnetic activity (Sandford, 1968; Feldstein & Galperin, 1985). Work by Sandford (1968) showed that during solar maximum, diffuse aurora accounts for 80% of auroral emission, however during solar minimum that was reduced to only 50%. While discrete aurora are much brighter and better known, diffuse aurora play an important role in the magnetosphere - ionosphere (MI) system because they are so common and thus are one of the largest sources of energy transfer between the two regions of geospace (Newell et al., 2009). The glow of diffuse aurora is the result of 100s of eV to 10s of keV electron precipitation from the plasma sheet (Meng et al., 1979). Many studies have identified wave-particle interactions in the plasma sheet as the primary way that this precipitation occurs. The waves responsible are electron cyclotron harmonic (ECH) and upper-band chorus (UBC) waves (e.g., Meredith et al., 2009; Thorne et al., 2010; Ni et al., 2016, and others). ECH waves are electrostatic perturbations whose frequencies fall between harmonics of the electron gyrofrequency (f_{ce}) (e.g., Kennel et al., 1970; Fredricks & Scarf, 1973; Shaw & Gurnett, 1975; Gurnett et al., 1979, and others). UBC waves are electromagnetic and a subset of whistler mode chorus waves with frequencies between $0.5f_{ce} < f < f_{ce}$ (e.g., Tsurutani & Smith, 1974; Burtis & Helliwell, 1976, and others). They differ from lower-band chorus (LBC) waves, which cover the frequency range $0.1f_{ce} < f < 0.5f_{ce}$. ECH and UBC waves also scatter slightly different energy electrons. ECH are most efficient between a few hundred eV to a few keV while chorus are most efficient below a few hundred eV (Horne et al., 2003). While most studies have linked ECH and UBC waves as the primary source of diffuse aurora, there is also a case to be made for whistler mode hiss waves, which have frequencies below $0.1f_{ce}$. These waves resonate best with electrons of energies above a few keV (Horne et al., 2003).

Despite their usual static appearance, diffuse aurora can vary on smaller scales, which is often referred to as structured diffuse aurora (SDA). Nightside SDA manifests as regular, parallel auroral stripes, brighter than the background (Sergienko et al., 2008). Sergienko et al. (2008) found that SDA is caused by precipitating electrons above 3-4 keV and linked these to whistler mode hiss waves. Diffuse aurora also often occur alongside the more dynamic pulsating aurora (Davis, 1978). Pulsating aurora are characterized by widely varying diffuse-like patches that blink on and off with periods between 2 to 20 seconds (e.g., Davis, 1978; Lessard, 2012, and others) and can be widespread and long-lasting (Jones et al., 2013). While they frequently happen during diffuse aurora, studies have shown that pulsating aurora originate from a different wave-particle interaction. This interaction happens in the outer radiation belt between LBC waves and a few to 100s of keV electrons (e.g., Nishimura et al., 2010, 2011; Jaynes et al., 2013; Kasahara et al., 2018). Another, less studied, phenomenon associated with diffuse aurora is black aurora. These are defined regions within an auroral patch that have no emissions (Davis, 1978; Trondsen & Cogger, 1997). The exact cause of these aurora is still unknown.

Both pulsating aurora and black aurora appear in the data set we analyzed, but our focus was on an entirely new phenomenon, seemingly associated with SDA. The events appear in images taken the night of March 15, 2002, during a campaign in Churchill, MB, Canada. These images demonstrate periods in which localized pulsations "black out" the diffuse glow, which then fills in over several seconds. We refer to this phenomenon as a diffuse auroral "eraser". This new auroral feature is worth investigating since it could lead to a better understanding of diffuse aurora. What process in the equatorial magnetosphere can turn off diffuse auroral emissions in localized patches?

2 Data

The images used in this analysis were taken from an intensified, narrow field-of-view (FOV) CCD-based TV camera known as the Portable Auroral Imager (PAI) (Trondsen & Cogger, 1997). They were taken at 30 frames-per-second (fps) and span from approximately 6:40 to 8:40 universal time (UT) or 0:06 to 2:06 magnetic local time (MLT) on March 15, 2002. The PAI was mounted to a tripod, which was on the ground at a location near Churchill, Manitoba. This corresponds to 69.28° latitude and 331.22° longitude in AACGM coordinates. It was pointed manually during the nightly observations and equipped with a 25 mm lens in addition to a Wratten 89B IR filter with a cutoff wavelength of 650 nm. Trondsen (1998) describes the PAI used to collect the data in more detail. This setup resulted in a 30.9° by 23.2° FOV. Given an image size of 640 by 480 pixels, the single pixel resolution is 88 m by 88 m at an altitude of 105 km (Trondsen, 1998). Using a section of Ursa Major that was visible in the images, we were able to es-

Figure 1. An unprocessed image from the original data. The first several seconds of the video include a UT timestamp. Ursa Major appears at the top of the image.

timate that the PAI was facing south of zenith, spanning elevation angles between 66.8° and 90°. Figure 1 is an example of one of the raw images. To reduce data size and improve image quality, we averaged every 10 frames to produce a 3 fps video, which we then analyzed. Our analysis of this data is a continuation of preliminary work by Jaynes (2013).

3 Case Study

To better describe this phenomenon we first investigate a single representative event (number 28 from the list of 32 events as identified in Figure 4). Figure 2 shows three images taken at different times during this event. We changed the contrast and color map of the images to see the event better. In the first image the aurora begins as a diffuse background. In the second image structured diffuse aurora appears in the form of a brighter stripe in the lower third of the frame. By the third image, the stripe has disappeared and the background aurora is darker than before, as if someone has taken an eraser to

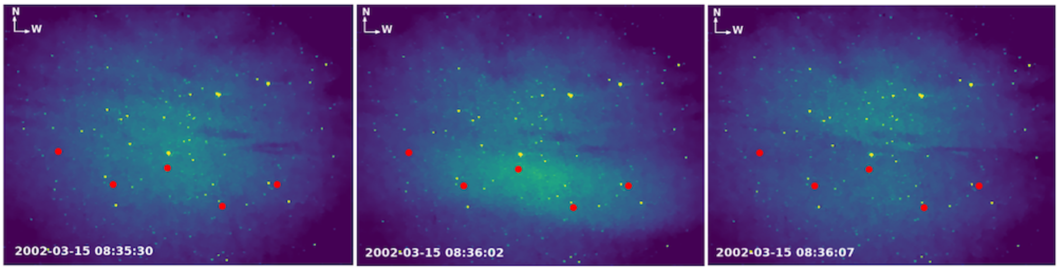

Figure 2. Images across a characteristic eraser event. From left to right the images are before the event, during the event brightening, and during the event eraser. The red dots indicate the 5 pixels we used to represent the event.

it. Small black auroral forms can also be seen in each frame, although we do not explore those features in this paper.

To represent the event, we picked 5 pixels from across the image frame. These are represented by the red dots in Figure 2. By taking the median of a 5x5 pixel block centered on each of those, and then the average of the 5 block values, we were able to estimate the brightness of the event at each time step. Figure 3 shows this brightness plotted versus time after applying a 1.5 second smoothing window. In addition, Figure 3 is color coded to indicate what we refer to as the 4 phases of an auroral eraser event. The initial phase (solid green) is the period before the event with a uniform diffuse aurora background. The brightening phase (dotted red) comes next and is characterized by a stripe of aurora that rapidly brightens. Shortly after, the brighter section disappears in the eraser phase (solid black), taking the diffuse background with it. Finally, in the recovery phase (dotted purple) the pixels return to their original brightness over several tens of seconds. For this event, the recovery time is 32 seconds. The details of how this is calculated are in the next section.

4 Analysis

We found that the best way to identify an auroral eraser event was in a keogram. This is a type of figure that is often used to visualize the evolution of aurora. We constructed ours by setting each keogram column to the median of the 21 center columns of the corresponding image frame. Initially, we split the data into 20 minute sections, to limit the size, and made a keogram for each. We found auroral eraser events in only

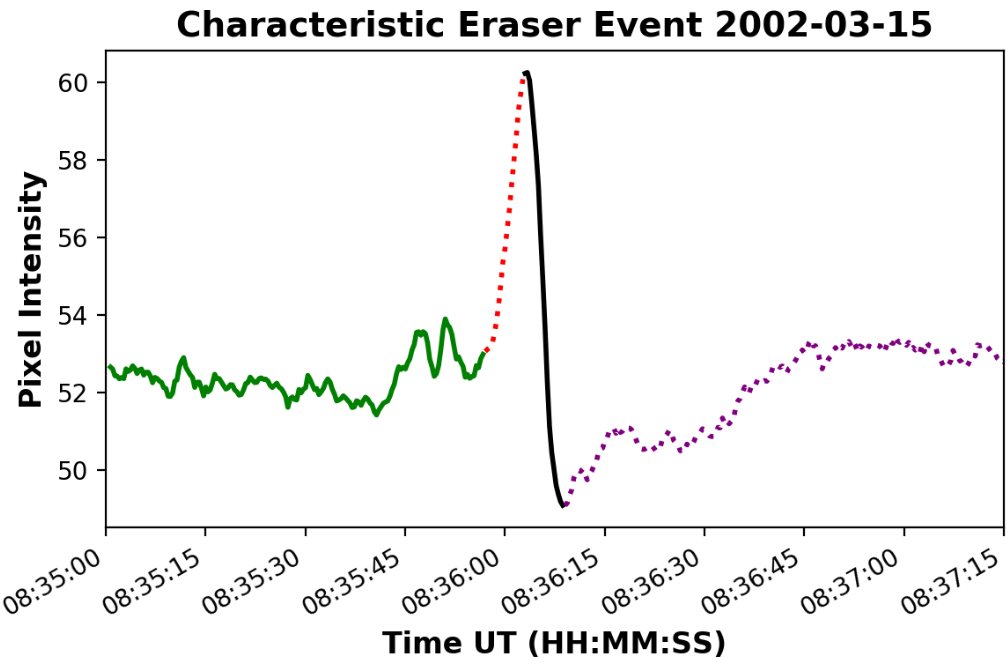

Figure 3. The averaged intensity of a characteristic eraser event. The event is color coded by phase: initial (solid green), brightening (dotted red), eraser (solid black), recovery (dotted purple).

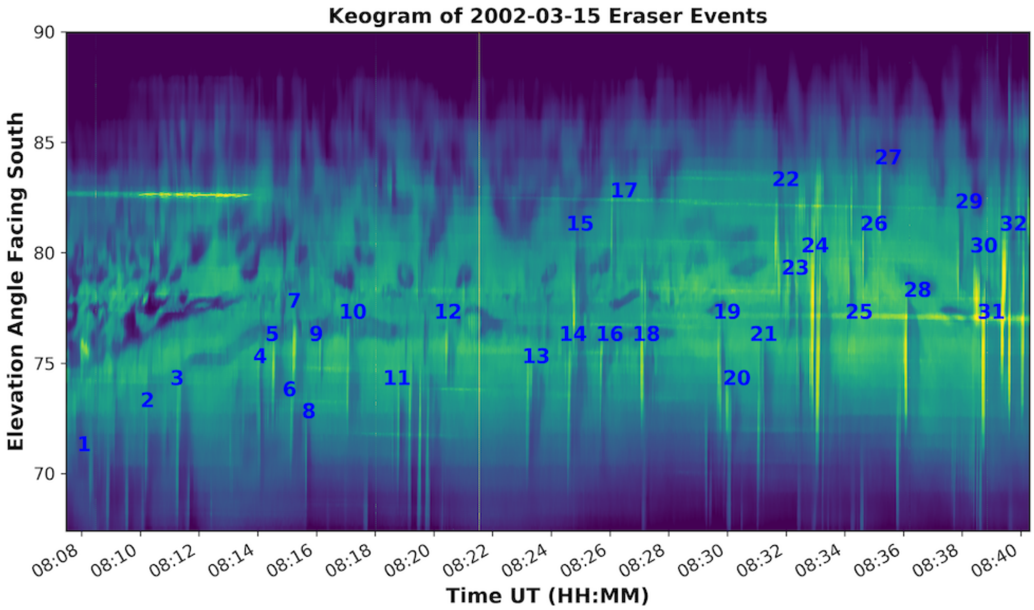

Figure 4. A keogram from the end of the data. This includes all of the auroral eraser events we identified. We increased the contrast and used the Viridis color map to see the events better.

the last 2, so we combined these to create Figure 4. The 32 events we found are labeled in the figure. These are identifiable by a bright vertical strip, followed by a darker section. An observant reader might also notice darker patches scattered across the keogram in addition to the auroral erasers. These are black aurora, which we mention, but did not study further. Finally, the bright horizontal streaks are stars that happened to fall within the center columns of the base images.

Using the keogram to identify all of the events, we then created an intensity versus time plot, like Figure 3, for each auroral eraser. Looking at these plots, it was clear that some events didn't have a full recovery phase, often being disrupted by a second event (see Figure 8 as an example). From the 32 events, we were able to visually identify 22 with recoveries that were not interrupted by a second event. Using these, we performed a superposed epoch analysis, shown in Figure 5. We set an epoch time halfway between the peak of the brightening phase and the trough of the eraser phase. We also normalized the pixel intensity by setting the average of the initial phase to zero. The time range associated with this was 100 to 30 frames or 43 to 10 seconds before the epoch. We could then determine the time from trough of the eraser phase to when the brightness returned to zero, we called this the recovery time. The average recovery time from this analysis

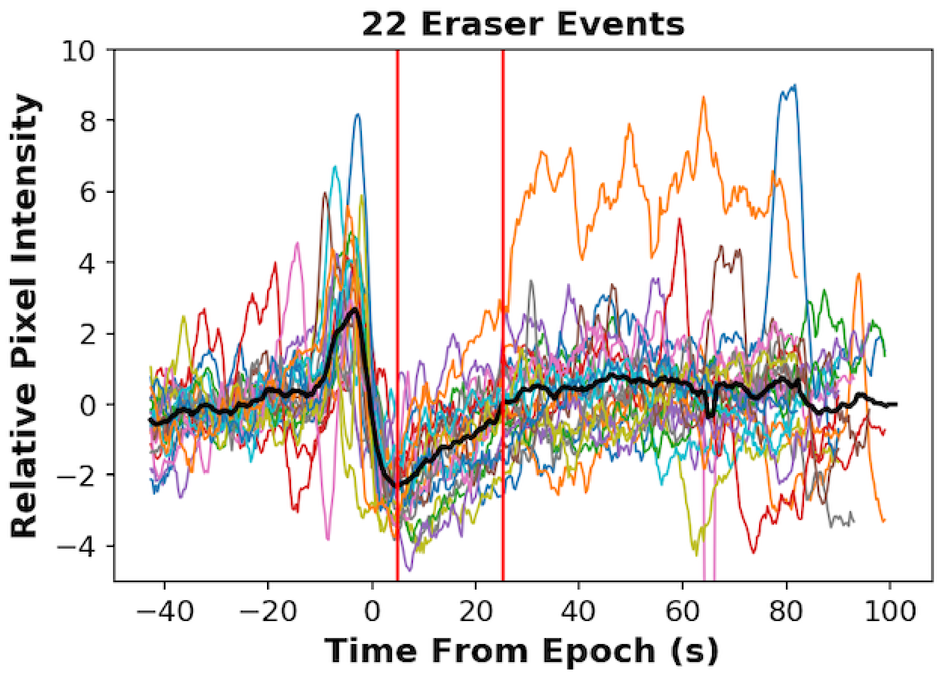

Figure 5. Epoch analysis for the 22 eraser events with a full recovery. The red lines indicate the start and stop of the average recovery period, which is 20 seconds.

was 20 seconds. However, the standard deviation was 13.17 seconds, highlighting that individual events can vary dramatically. This can be further seen in Figure 6, which is a histogram of the recovery times from the 22 events. The large peak for times less than 10 seconds is a result of events whose initial phases slowly increase in brightness instead of remaining constant. This causes the baseline average to be lower than other events.

We were also interested in the magnetic conditions on March 15, 2002. To learn about these we looked at several different sources. The solar wind speed as extracted from NASA/GSFC's OMNI data set through OMNIWeb, was between 340 and 360 km/s. OMNI is a database of combined solar wind parameters from multiple spacecraft including WIND and ACE. B_z ranged between 0 and 6 nT, and the KP index was $<$ 2 (King & Papitashvili, 2005). In all, the solar wind conditions were unremarkable and indicated low magnetic activity. The story was the same for ground-based magnetometers. SuperMAG is a database of over 300 magnetometers, each of which measures magnetic fields in 3 directions (Gjerloev, 2009, 2012). We looked at data from several stations during the night of March 15, 2002. Data from Churchill (FCC) and surrounding magnetometers (IQA,

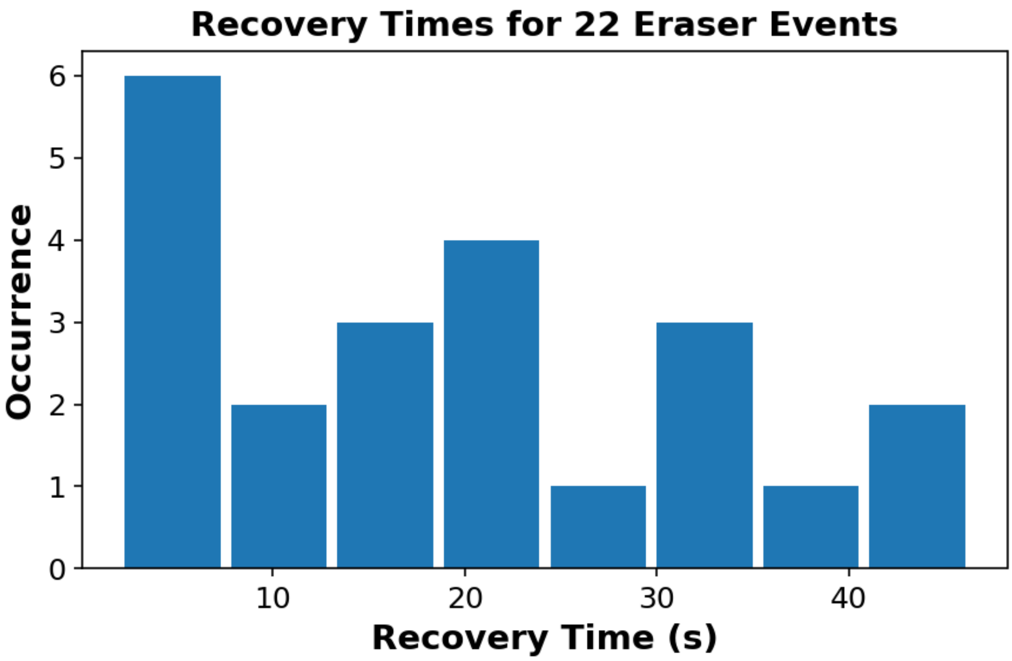

Figure 6. Histogram of the recovery times for the 22 eraser events with a full recovery. The recovery time is calculated as the time between the end of the eraser phase to when the brightness returns to the average of 43 seconds to 10 seconds before the brightening phase.

SKT) showed no major perturbations in any of the field directions. Magnetometers on the north-east coast of Greenland and on Svalbard (DNB, NAL) did show some activity in the form of small wave-like fluctuations. These are plotted in Figure 7. Unfortunately, the highest fidelity option was 1 minute, so we were unable to see any higher frequency modulations. Finally, the Auroral Electrojet (AE) index, which is derived from the horizontal component of select magnetometers around the globe, indicated low magnetic activity with a value of < 90 nT.

5 Discussion

These events appear to be associated with structured diffuse aurora (SDA) forms, but to our knowledge, an event such as this has not been reported on in the scientific literature. This is intriguing as the global and local geomagnetic data we investigated appears to show ordinary conditions that likely occur frequently. Are eraser events such as these a common quiet time phenomenon and have other observations just overlooked them, or are they rare? Due to the narrow field-of-view and high sensitivity required to observe auroral eraser events, in addition to unpublished accounts of similar sightings, we believe they occur more frequently than the published work would indicate. However, it would be necessary to conduct a more detailed search to answer this question.

Events showing atypical fluctuations in brightness have been published on before. Dahlgren et al. (2017) mentions observing a dip in brightness, to below the average, during the off phase of pulsating aurora. While this is similar, the lack of pulsating aurora in our observations suggests that they are different phenomena. A type of aurora known as dual-layer pulsating aurora could also be similar (Royrvik, 1976; Trondsen & Cogger, 1997). Trondsen and Cogger (1997) described it as a section of foreground diffuse aurora that turns off, revealing a background with structure in it. It is possible that these are auroral eraser events, but the difference in camera setup make it difficult to tell.

Without concurrent in situ spacecraft observations, we can only speculate on a possible driver of these features. One possible cause could be specific wave-particle interactions, since diffuse aurora are associated with both electron cyclotron harmonic (ECH) waves and chorus waves. As Ni et al. (2011) showed, the scattering efficiencies are different between ECH and chorus waves for different pitch angle particles. Chorus waves scatter more efficiently over a wider pitch angle distribution than ECH waves. If, dur-

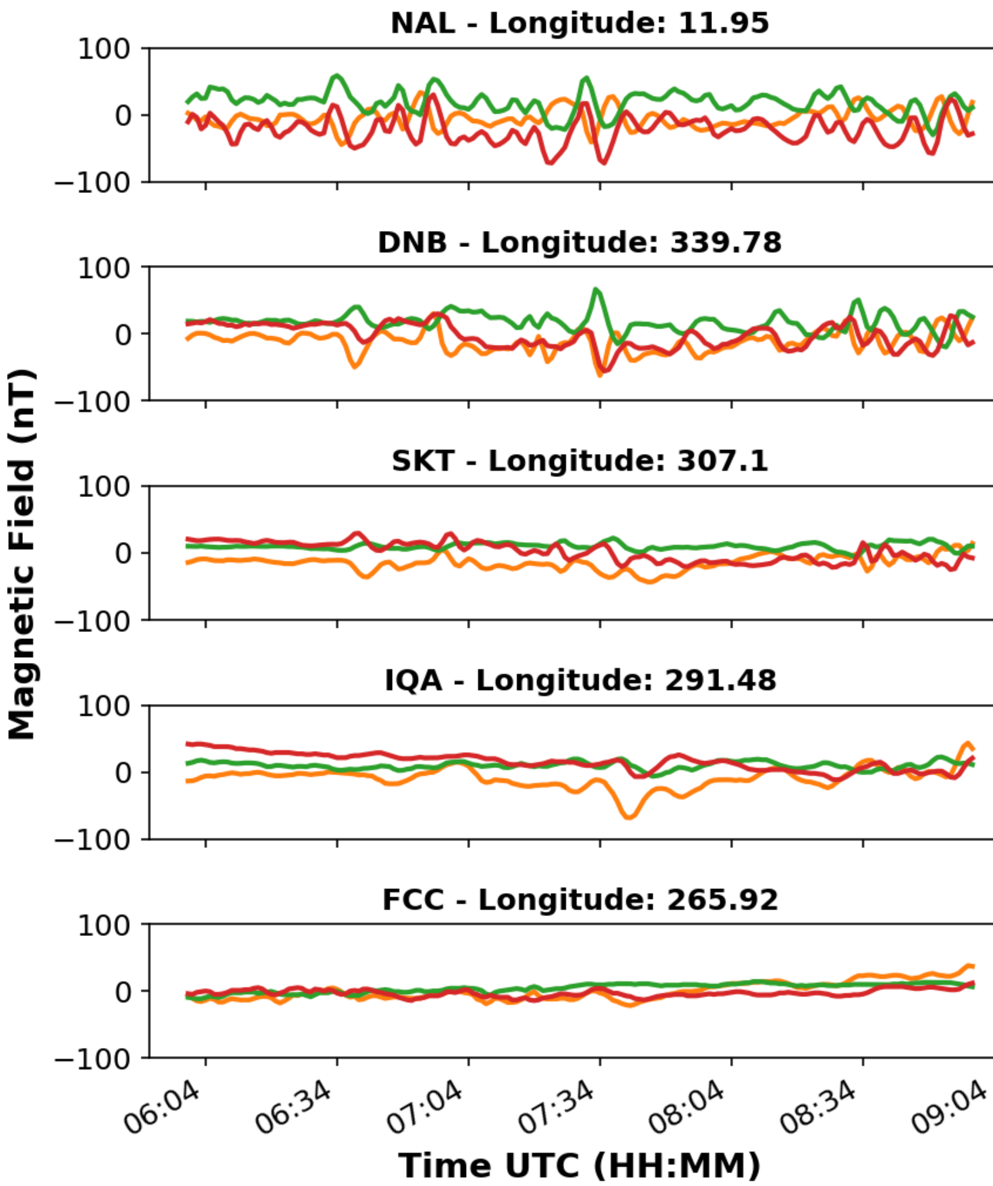

Figure 7. Five ground-based magnetometers during the night of March 15, 2002. The plots are arranged by eastward geographic longitude from bottom to top. The bottom three are located between Churchill and the west coast of Greenland. The top two are located on the east coast of Greenland and on Svalbard.

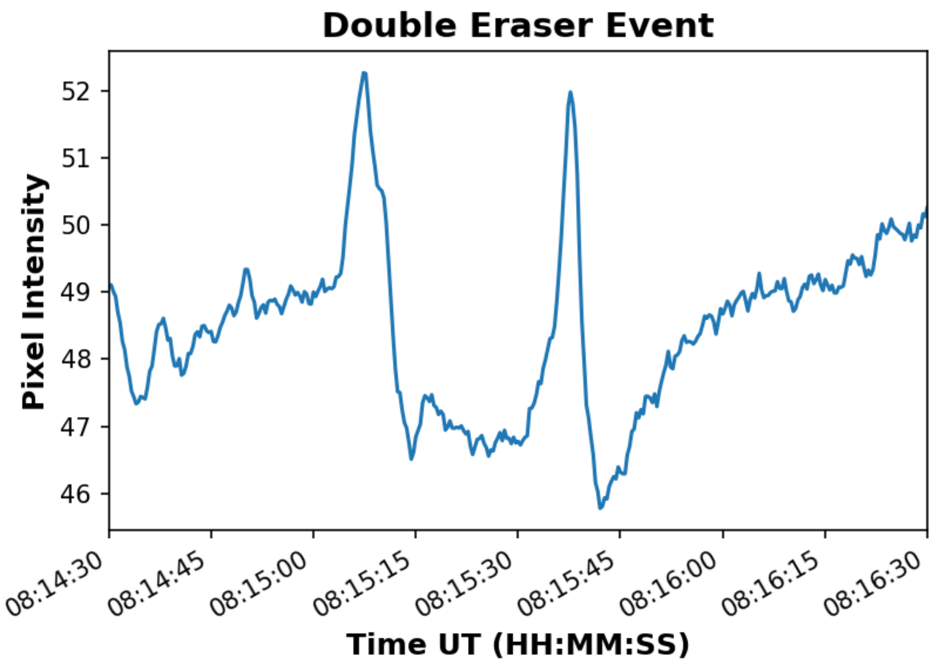

Figure 8. Event 28 begins as a normal eraser event, but before the diffuse background is able to fully refill, a second events appears to occur. After this the background refills as normal.

ing an instance of ECH driven diffuse aurora, a packet of chorus waves passed through the region, the effect might be to momentarily increase the electron flux, causing the brightening we observe. If the chorus waves were strong enough they could deplete electrons in the narrower ECH pitch angle scattering distribution, causing the eraser. If this were true, we would expect a second peak if a second packet of chorus waves passed through the region before the diffuse aurora had completely recovered. We see this behavior in several cases as Figure 8 shows. This is further backed up by observations of coupling between the upper and lower sidebands of ECH waves and chorus waves by Gao et al. (2018), as well as the theorized cause of structured diffuse aurora in Sergienko et al. (2008). However, this explanation is only speculative and we would need more detailed modeling to determine if this is truly a possible driver.

6 Summary

- A diffuse auroral eraser event is characterized by an initial background of diffuse aurora, followed by the brightening of a more defined structured aurora stripe, which disappears and takes the background aurora with it. The background then refills back to the initial state at a slower rate. This recovery time can vary dramatically, but averages around 20 seconds.

- The eraser events we observed occurred within diffuse aurora and during times of low magnetic activity. In addition, they all occurred within 40 minutes of each other.
- From our knowledge there have been no other reports of events such as these, which raises the question: are these a common quite time phenomenon that has been overlooked or are they rare?

Acknowledgments

Imager data referenced in this paper is available from Knudsen et al. (2002).

Participation of DK in the March 2002 Churchill campaign was supported by the Natural Science and Engineering Council of Canada (NSERC). Participation of TT was supported by an NSERC grant held by LL Cogger. Participation of SJ was supported by Dartmouth College's Women in Science Project.

We acknowledge use of NASA/GSFC's Space Physics Data Facility's OMNIWeb service, and OMNI data. The Dst and AE indices were provided by World Data Center C2, Kyoto University, Japan. We gratefully acknowledge the SuperMAG collaborators (http://supermag.jhuapl.edu/info/?page=acknowledgement) for providing the magnetometer data.

References

Burtis, W. J., & Helliwell, R. A. (1976, November). Magnetospheric chorus: Occurrence patterns and normalized frequency. *Planetary and Space Science*, *24*(11), 1007,IN1,1011-1010,IN4,1024. doi: 10.1016/0032-0633(76)90119-7

Dahlgren, H., Lanchester, B. S., Ivchenko, N., & Whiter, D. K. (2017, March). Variations in energy, flux, and brightness of pulsating aurora measured at high time resolution. *Annales Geophysicae*, *35*(3), 493-503. doi: 10.5194/angeo-35-493-2017

Davis, T. N. (1978, January). Observed microstructure of auroral forms. *Journal of Geomagnetism and Geoelectricity*, *30*(4), 371-380. doi: 10.5636/jgg.30.371

Feldstein, Y. I., & Galperin, Y. I. (1985, August). The auroral luminosity structure in the high-latitude upper atmosphere: its dynamics and relationship to the large-scale structure of the earth's magnetosphere. *Reviews of Geophysics*, *23*, 217-275. doi: 10.1029/RG023i003p00217

Fredricks, R. W., & Scarf, F. L. (1973, January). Recent studies of magnetospheric electric field emissions above the electron gyrofrequency. *Journal of Geophysical Research (Space Physics)*, *78*(1), 310-314. doi: 10.1029/JA078i001p00310

Gao, Z., Su, Z., Xiao, F., Summers, D., Liu, N., Zheng, H., ... Wang, S. (2018, December). Nonlinear Coupling Between Whistler-Mode Chorus and Electron Cyclotron Harmonic Waves in the Magnetosphere. *Geophysical Research Letters*, *45*(23), 12,685-12,693. doi: 10.1029/2018GL080635

Gjerloev, J. W. (2009, July). A Global Ground-Based Magnetometer Initiative. *EOS Transactions*, *90*(27), 230-231. doi: 10.1029/2009EO270002

Gjerloev, J. W. (2012, September). The SuperMAG data processing technique. *Journal of Geophysical Research (Space Physics)*, *117*(A9), A09213. doi: 10.1029/2012JA017683

Gurnett, D. A., Anderson, R. R., Tsurutani, B. T., Smith, E. J., Paschmann, G., Haerendel, G., ... Russell, C. T. (1979, December). Plasma wave turbulence at the magnetopause: Observations from ISEE 1 and 2. *Journal of Geophysical Research (Space Physics)*, *84*(A12), 7043-7058. doi: 10.1029/JA084iA12p07043

Horne, R. B., Thorne, R. M., Meredith, N. P., & Anderson, R. R. (2003, July). Diffuse auroral electron scattering by electron cyclotron harmonic and whistler mode waves during an isolated substorm. *Journal of Geophysical Research (Space Physics)*, *108*(A7), 1290. doi: 10.1029/2002JA009736

Jaynes, A. N. (2013). *Pulsating Aurora: Source Region and Morphology (Doctoral dissertation)* (Unpublished doctoral dissertation). University of New Hampshire.

Jaynes, A. N., Lessard, M. R., Rodriguez, J. V., Donovan, E., Loto'Aniu, T. M., & Rychert, K. (2013, August). Pulsating auroral electron flux modulations in the equatorial magnetosphere. *Journal of Geophysical Research (Space Physics)*, *118*(8), 4884-4894. doi: 10.1002/jgra.50434

Jones, S. L., Lessard, M. R., Rychert, K., Spanswick, E., Donovan, E., & Jaynes, A. N. (2013, June). Persistent, widespread pulsating aurora: A case study.

Journal of Geophysical Research (Space Physics), *118*(6), 2998-3006. doi: 10.1002/jgra.50301

Kasahara, S., Miyoshi, Y., Yokota, S., Mitani, T., Kasahara, Y., Matsuda, S., ... Shinohara, I. (2018, February). Pulsating aurora from electron scattering by chorus waves. *Nature*, *554*(7692), 337-340. doi: 10.1038/nature25505

Kennel, C. F., Scarf, F. L., Fredricks, R. W., McGehee, J. H., & Coroniti, F. V. (1970, November). VLF electric field observations in the magnetosphere. *Journal of Geophysical Research (Space Physics)*, *75*(31), 6136-6152. doi: 10.1029/JA075i031p06136

King, J. H., & Papitashvili, N. E. (2005, February). Solar wind spatial scales in and comparisons of hourly Wind and ACE plasma and magnetic field data. *Journal of Geophysical Research (Space Physics)*, *110*(A2), A02104. doi: 10.1029/2004JA010649

Knudsen, D. J., Troyer, R. N., Jaynes, A. N., Jones, S. L., & Trondsen, T. (2002). *Churchill Diffuse Auroral Campaign Tape-18 2002-03-15.* `https://zenodo.org/record/3911377#.XvosHC2z3mE`. doi: 10.5281/zenodo.3911376

Lessard, M. R. (2012). A review of pulsating aurora. In *Auroral phenomenology and magnetospheric processes earth and other planets* (Vol. 197, pp. 5673–68). Washington, D.C. :: American Geophysical Union.

Lui, A. T. Y., Perreault, P., Akasofu, S. I., & Anger, C. D. (1973, May). The diffuse aurora. *Planetary and Space Science*, *21*(5), 857,IN7,859-858,IN16,861. doi: 10.1016/0032-0633(73)90102-5

Meng, C. I., Mauk, B., & McIlwain, C. E. (1979, June). Electron precipitation of evening diffuse aurora and its conjugate electron fluxes near the magnetospheric equator. *Journal of Geophysical Research*, *84*(A6), 2545-2558. doi: 10.1029/JA084iA06p02545

Meredith, N. P., Horne, R. B., Thorne, R. M., & Anderson, R. R. (2009, July). Survey of upper band chorus and ECH waves: Implications for the diffuse aurora. *Journal of Geophysical Research (Space Physics)*, *114*(A7), A07218. doi: 10.1029/2009JA014230

Newell, P. T., Sotirelis, T., & Wing, S. (2009, September). Diffuse, monoenergetic, and broadband aurora: The global precipitation budget. *Journal of Geophysical Research (Space Physics)*, *114*(A9), A09207. doi: 10.1029/2009JA014326

Ni, B., Thorne, R. M., Meredith, N. P., Horne, R. B., & Shprits, Y. Y. (2011, April). Resonant scattering of plasma sheet electrons leading to diffuse auroral precipitation: 2. Evaluation for whistler mode chorus waves. *Journal of Geophysical Research (Space Physics)*, *116*(A4), A04219. doi: 10.1029/2010JA016233

Ni, B., Thorne, R. M., Zhang, X., Bortnik, J., Pu, Z., Xie, L., ... Gu, X. (2016, April). Origins of the Earth's Diffuse Auroral Precipitation. *Space Science Reviews*, *200*(1-4), 205-259. doi: 10.1007/s11214-016-0234-7

Nishimura, Y., Bortnik, J., Li, W., Thorne, R. M., Chen, L., Lyons, L. R., ... Auster, U. (2011, November). Multievent study of the correlation between pulsating aurora and whistler mode chorus emissions. *Journal of Geophysical Research (Space Physics)*, *116*(A11), A11221. doi: 10.1029/2011JA016876

Nishimura, Y., Bortnik, J., Li, W., Thorne, R. M., Lyons, L. R., Angelopoulos, V., ... Auster, U. (2010, October). Identifying the Driver of Pulsating Aurora. *Science*, *330*(6000), 81. doi: 10.1126/science.1193186

Royrvik, O. (1976). *Pulsating aurora: Local and global morphology* (Unpublished doctoral dissertation). Alaska Univ., College.

Sandford, P. B. (1968, December). Variations of auroral emissions with time, magnetic activity and the solar cycle. *Journal of Atmospheric and Terrestrial Physics*, *30*(12), 1921-1942. doi: 10.1016/0021-9169(68)90001-9

Sergienko, T., Sandahl, I., Gustavsson, B., Andersson, L., Brändström, U., & . Steen, Å. (2008, October). A study of fine structure of diffuse aurora with ALIS-FAST measurements. *Annales Geophysicae*, *26*(11), 3185-3195. doi: 10.5194/angeo-26-3185-2008

Shaw, R. R., & Gurnett, D. A. (1975, November). Electrostatic noise bands associated with the electron gyrofrequency and plasma frequency in the outer magnetosphere. *Journal of Geophysical Research (Space Physics)*, *80*(31), 4259. doi: 10.1029/JA080i031p04259

Thorne, R. M., Ni, B., Tao, X., Horne, R. B., & Meredith, N. P. (2010, October). Scattering by chorus waves as the dominant cause of diffuse auroral precipitation. *Nature*, *467*(7318), 943-946. doi: 10.1038/nature09467

Trondsen, T. S. (1998). *High Spatial and Temporal Resolution Auroral Imaging (Doctoral dissertation)* (Doctoral dissertation, University of Tromsø). Retrieved June 2020, from `https://www.researchgate.net/publication/`

277294393_High_Spatial_and_Temporal_Resolution_Auroral_Imaging_-_PhD_Dissertation

Trondsen, T. S., & Cogger, L. L. (1997, January). High-resolution television observations of black aurora. *Journal of Geophysical Research*, *102*(A1), 363-378. doi: 10.1029/96JA03106

Tsurutani, B. T., & Smith, E. J. (1974, January). Postmidnight chorus: A substorm phenomenon. *Journal of Geophysical Research (Space Physics)*, *79*(1), 118-127. doi: 10.1029/JA079i001p00118

Figure 1.


T 06:37:23:17

Figure 2.

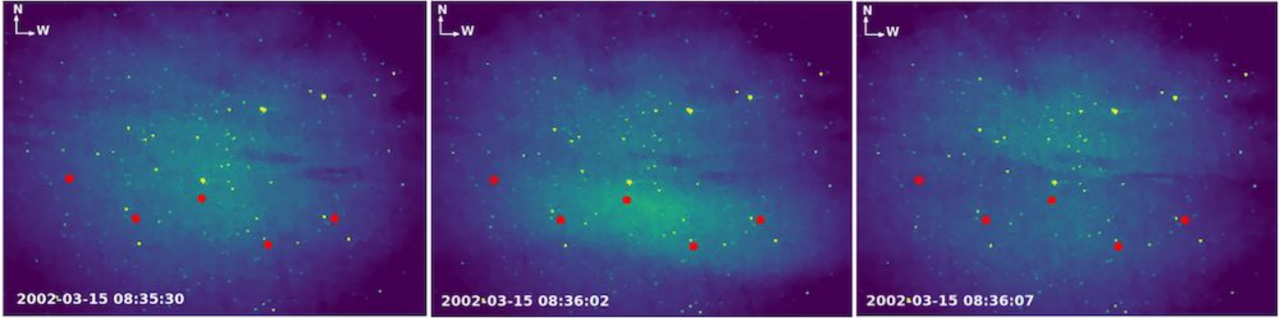
N
W
2002-03-15 08:35:30
N
W
2002-03-15 08:36:02
N
W
2002-03-15 08:36:07

Figure 3.

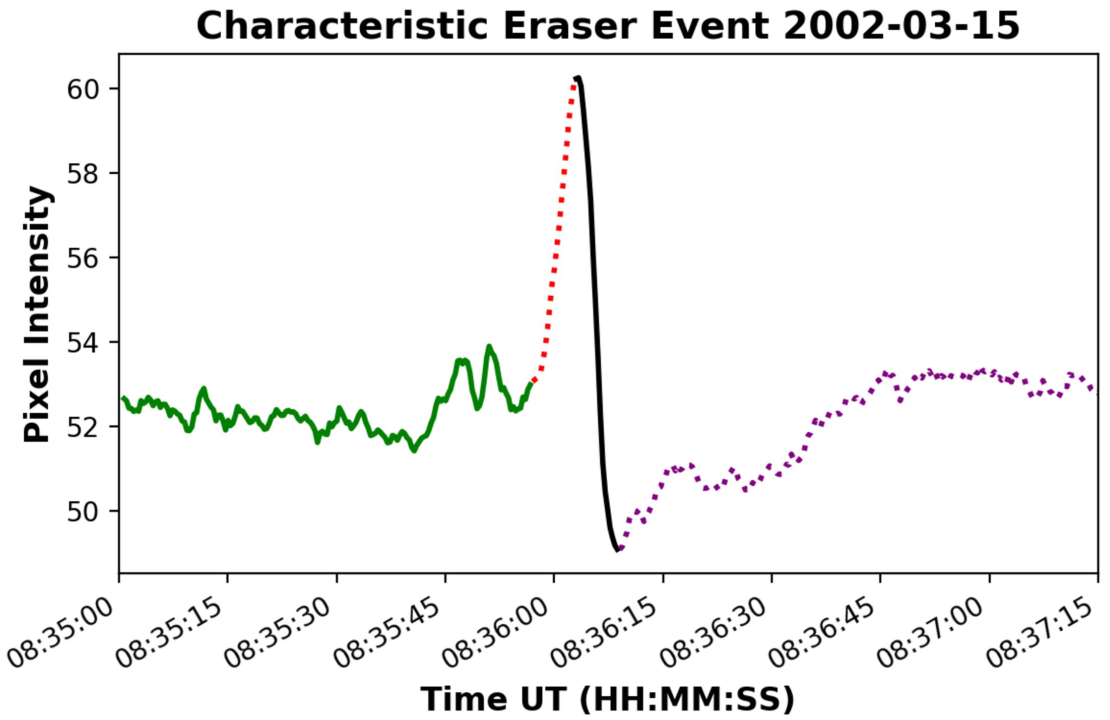

Characteristic Eraser Event 2002-03-15
Pixel Intensity
60
58
56
54
52
50
08:35:00
08:35:15
08:35:30
08:35:45
08:36:00
08:36:15
08:36:30
08:36:45
08:37:00
08:37:15
Time UT (HH:MM:SS)

Figure 4.

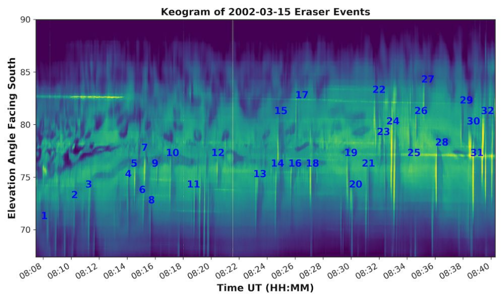

Keogram of 2002-03-15 Eraser Events
Elevation Angle Facing South
90
85
80
75
70
08:08
08:10
08:12
08:14
08:16
08:18
08:20
08:22
08:24
08:26
08:28
08:30
08:32
08:34
08:36
08:38
08:40
Time UT (HH:MM)
1
2
3
4
5
6
7
8
9
10
11
12
13
14
15
16
17
18
19
20
21
22
23
24
25
26
27
28
29
30
31
32

Figure 5.

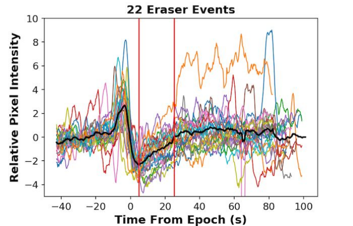

22 Eraser Events
Relative Pixel Intensity
Time From Epoch (s)
10
8
6
4
2
0
−2
−4
−40
−20
0
20
40
60
80
100

Figure 6.

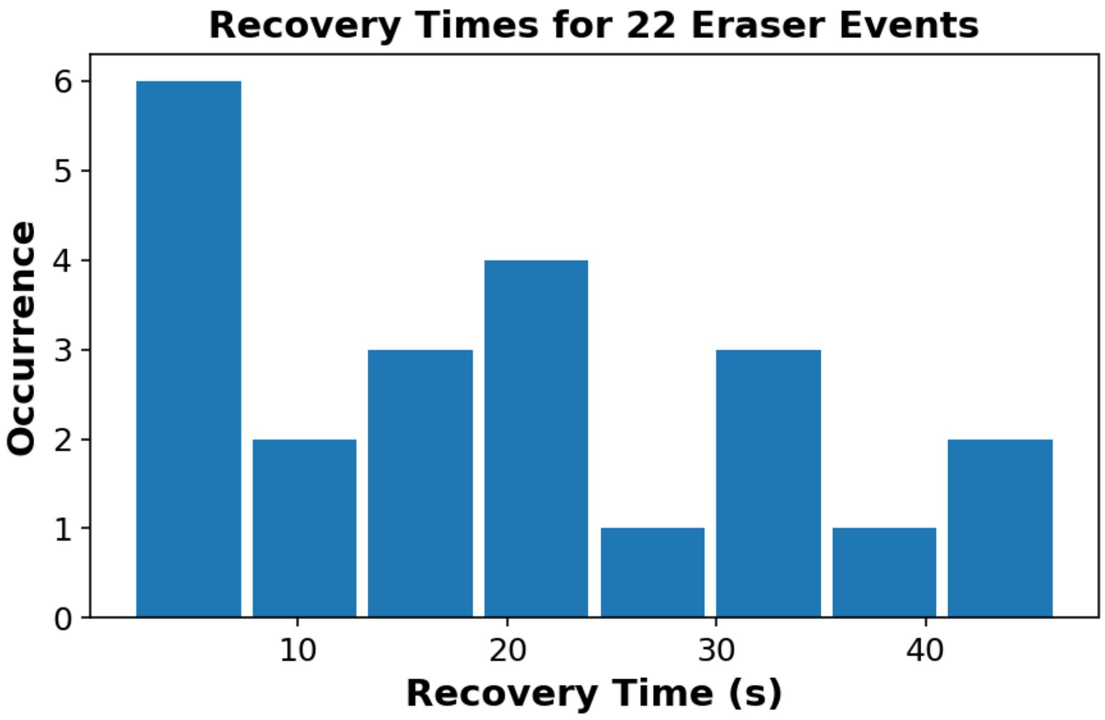

Recovery Times for 22 Eraser Events
Occurrence
Recovery Time (s)
0
1
2
3
4
5
6
10
20
30
40

Figure 7.

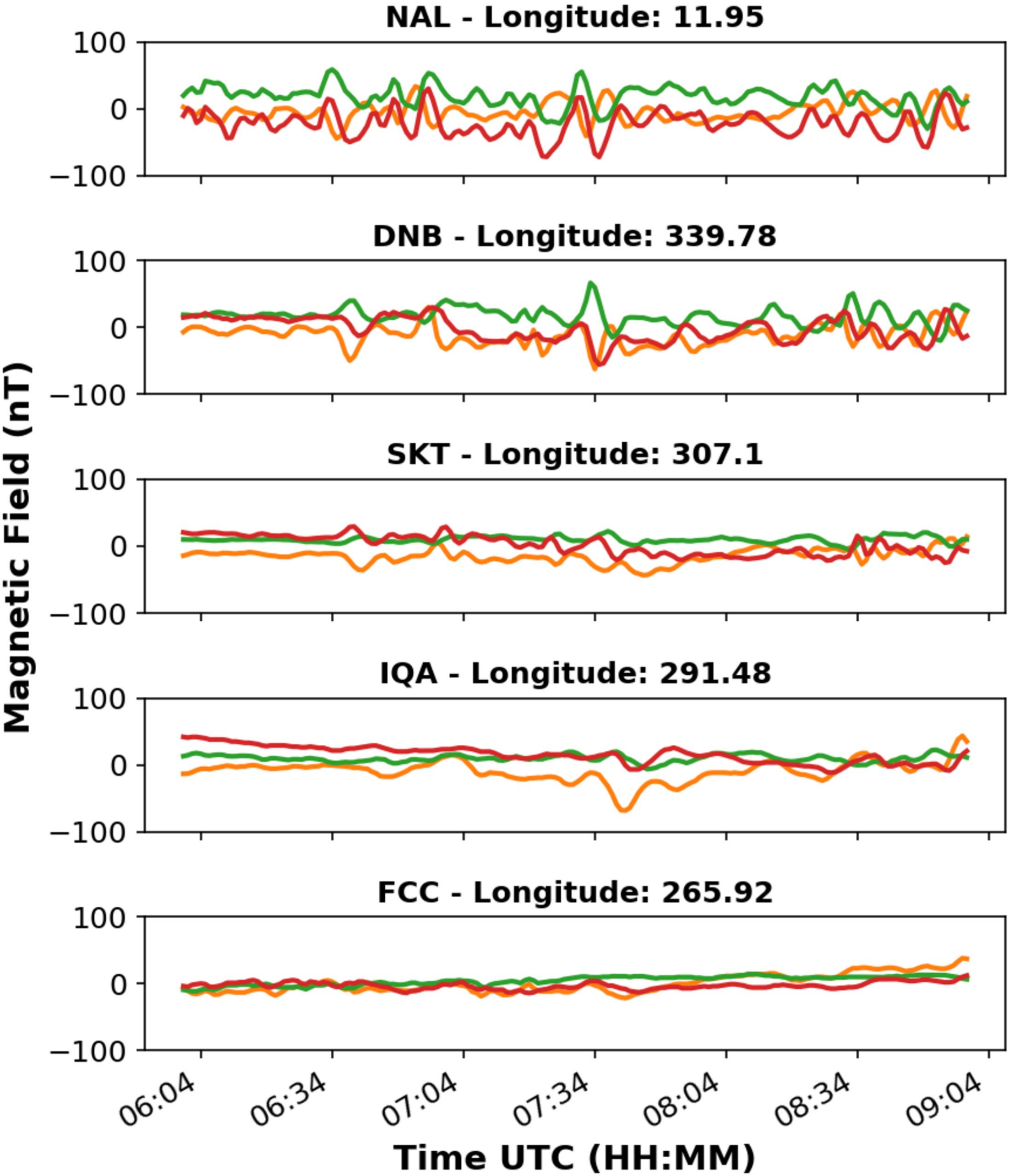
NAL - Longitude: 11.95
DNB - Longitude: 339.78
SKT - Longitude: 307.1
IQA - Longitude: 291.48
FCC - Longitude: 265.92
100
0
−100
Magnetic Field (nT)
06:04
06:34
07:04
07:34
08:04
08:34
09:04
Time UTC (HH:MM)

Figure 8.

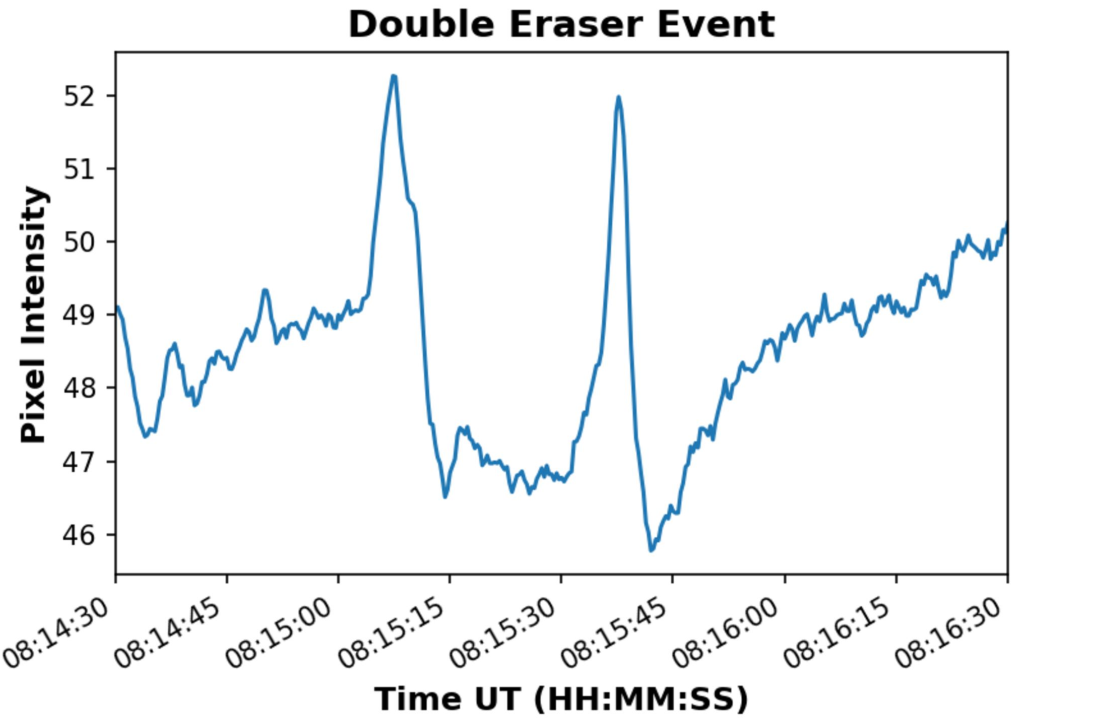
Double Eraser Event
Pixel Intensity
52
51
50
49
48
47
46
08:14:30
08:14:45
08:15:00
08:15:15
08:15:30
08:15:45
08:16:00
08:16:15
08:16:30
Time UT (HH:MM:SS)